Continuous Casting of Hypermonotectic AlBiZn Alloys: Experimental Investigations and Numerical Simulation

M. Gruber-Pretzler[1], F. Mayer[1], M. Wu[1], J. Moiseev[2], B. Tonn[2], A. Ludwig[1]
[1]University of Leoben, Leoben, Austria
[2]Clausthal University of Technology, Clausthal-Zellerfeld, Germany

1 Abstract

Hypermonotectic alloys separate into two melts prior to solidification. Therefore, continuous casting of hypermonotectic alloys is still a challenge that inhibits the use of these bearing materials in industry. As the secondary phase distribution has a major impact on the wear properties of the final product, it is of utmost importance to understand its formation. The motion of the secondary phase droplet during demixing of the melt is caused mainly by Marangoni transport and gravity-induced sedimentation. By a series of experiments with hypermonotectic AlBiZn alloys, a laboratory scale strip casting device has been adapted to the special behavior of these alloys. The resulting droplet distributions were experimentally investigated by varying not only the alloy composition but also relevant process parameters. Beside this investigation the formation of secondary phase distribution was also modeled with a two-phase volume averaging approach. The Bi-enriched minority liquid phase is treated as the second phase whereas the parent melt as first. The model solves the mass, momentum, species and enthalpy conservation equations for both liquids including droplet nucleation, solute redistribution and monotectic reaction.

2 Introduction

Alloys with a miscibility gap in the liquid state, especially for those with gross concentration above the monotectic point (hypermonotectics), are potential bearing materials for the automotive industry [1, 2]. As hypermonotectic alloys separate into two melts prior to solidification their continuous casting is still a challenge. Difficulties arise from the fact that the secondary phase droplets move due to Marangoni forces and gravity-induced sedimentation. After a period of less attention, the interest on the solidification of hypermonotectic alloys has increased again, because the EU has proscribed the use of Pb containing alloys. Therefore, the development of new Pb-free bearing materials is of great importance and so alloys based on Al-Bi are again of particular interest for materials research and development [3, 4].

Strips of hypermonotectic alloys are produced at the TU Clausthal on a vertical continuous casting unit at a laboratory scale. This unit insures the possibility of high cooling rates that are necessary for the casting of hypermonotectic alloys in order to cross the demixing interval very rapidly. Due to consequent prevention of minority-phase sedimentation, a fine distribution of Bi drops in the Al matrix can be produced. However, the influence of additional alloying elements, like Zn, or of differences in process parameters, like casting speed, casting temperature and cooling conditions on the distribution of the minority phase is still open and thus addressed in the present paper.

Theoretical descriptions of the demixing of hypermonotectic Al-based alloys were already suggested in [5–6]. A numerical treatment of this process was presented by two of the authors in 2003 [7, 8]. Their work addressed the influence of Marangoni force and of gravity-induced droplet sedimentation on the droplet distribution. However, the studies presented in [7, 8] were done for 2D square geometry which was assumed to be cooled from all sides. In the present study, a first numerical description of a strip casting process for the solidification of a hypermonotectic binary AlBi10 alloy is given. The temperature field and the distributions of droplet fraction and density are presented and discussed.

This paper consists of two parts, the first is the experimental part and the second the numerical part.

3 Experimental Part

3.1 Description of the Continuous Casting Unit

The vertical continuous casting machine at the TU Clausthal consists of the mold with pouring nozzle and tundish and the mechanical-hydraulic strand withdrawal mechanism. The ready-assembled continuous casting copper mold is made out of two side frames and two spacers. The spacers confine the strand laterally and keep the mold gap at a constant width of $\Delta = 10$ mm. A steel pouring nozzle is set into a notch at the top of the mold and a tundish symmetrically on top of that. Figure 1 illustrates schematically the assembled mold ready for use. The tundish (1) and the steel pouring nozzle (2) are pre-heated up to the pouring temperature. The melt is heated up in a separate furnace also to that temperature and then poured into the tundish in order to start the casting.

There are two cooling water circuits. In the first circuit the cooling water is flowing through the cooling water supply (5) towards the cooling channel (6) where the water directly impinges the strand (7). This cooling channel acts as secondary cooling, while the upper part of the mold operates as primary cooling. In each half of the mold there are a total of 17 cooling channels and associated cooling grooves. With the cooling circuit (4) an additional heat removal from the

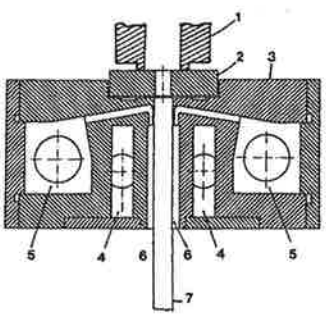

Figure 1: Scheme of the middle cross section through the mold (detailed information in the text and see ref. [9])

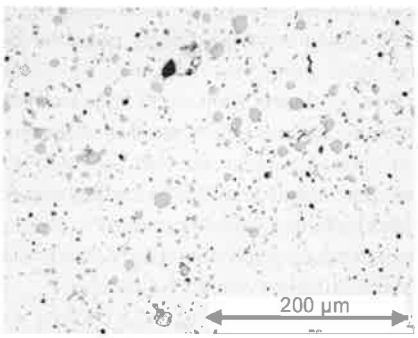

Figure 2: Bi droplets distribution in an $AlBi_8Zn_6$ strand

mold is realized. The amount of water flowing through the two cooling water circuits can be varied depending on the required cooling intensity. With the maximum cooling possible a temperature gradient at the solidification front of $G = 50$ K/mm [3]. Steady-state casting conditions are found to be reached after a few seconds. Therefore, a uniform phase distribution along the length and width of the strand can be established.

3.2 Evaluation and Discussion of Results

In the primary cooling zone which extends over the first $L = 23$ mm of the copper mold, the melt is cooling rapidly. When the temperature falls below the binodal temperature, droplets of the minority phase start to form. From the experimental point of view, it is obvious to assume that the main nucleation happens in areas close to the walls. Further growth the nucleated droplets is then governed by diffusion. Due to the Marangoni effect, which is caused by the temperature-dependence of the interfacial tension, the continually growing particles migrate towards the middle of the strand. This favors their collision and coagulation. The Marangoni force is proportional to the temperature gradient and proportional to the square of the droplet diameter, whereas the Stokes forces increases only linearly with the diameter. The occurring droplet motion is the overlay of casting flow, Marangoni motion and sedimentation.

Figure 2 gives a qualitative impression of the Bi-droplet distribution in the strand of $AlBi_8Zn_6$. The structural constituents occurring in this case were produced at a casting velocity of $V_{cast} = 450$ mm / min, a casting temperature of about $T_{cast} = 960$ °C and a cooling water flow rate of about $Q = 4000$ l/hour for each mold side frame. In all ternary Al-Zn-Bi alloys the edge strand zones are depleted in Bi-droplets up to a depth of 4 mm. In the Al-Bi system the monotectic composition occurs at $c_m = 3.4$ wt.% of bismuth. This composition corresponds approximately to the contents measured in the edge zones. In opposite, the core zone of the strand is enriched in droplets and reveals around twice as much as Bi content compared to the initial composition.

Figure 3 to 6 give an overview on the influence of variations in alloy composition and process parameters like casting speed, casting temperature or cooling water flow rate on the maximum and the mean Bi-droplet size. Figure 3 shows how the mean and maximum droplet size in the enriched middle zone by varying the Zn content for the two alloys, $AlBi_6Zn_x$ and $AlBi_8Zn_x$. Figure 4 shows the influence of the casting speed on the mean and maximum droplet size for the $AlBi_8Zn_6$ alloy.

It is visible that increasing Zn content increases the Bi-droplet size to a certain level for both, mean and maximum values. However, if the amount of Zn in the alloy is larger than 10 wt.% the droplet size decreases again. On the other side, high Bi amount leads to a clear increase of the droplet size. The influence of the Bi-content on the droplet size is substantially stronger than the one of Zn and higher radial components.

If a casting is desired which reveal only small size maximum droplets, the optimum casting speed for an $AlBi_8Zn_6$ alloy would be around $V_{cast} = 550$ mm/min. This finding is true for a casting temperature of $T_{cast} = 960$ °C and a cooling water flow rate of $Q = 4000$ l/hour. A small casting speed would favor the drop growth already in the steel feeder. Evidently, a larger casting speed would lead to a deep melt pool and thus higher temperature gradients in front of the solidification front. This increases the importance of the Marangoni convection and hence influences the appearing droplet distribution.

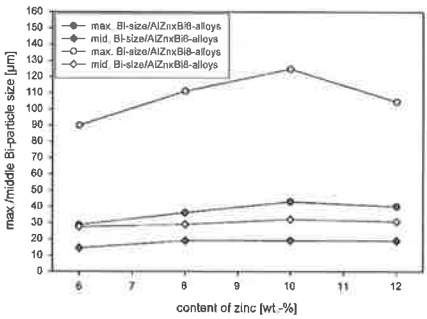

Figure 3: Influence of Zn- and Bi-content on the mean and maximum Bi-droplet size in $AlBi_8Zn_x$ and $AlBi_6Zn_x$

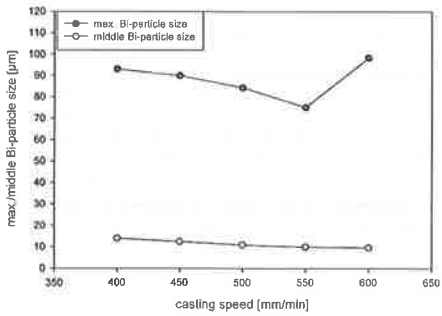

Figure 4: Influence of casting speed on the mean and maximum Bi-droplet in $AlBi_8Zn_6$

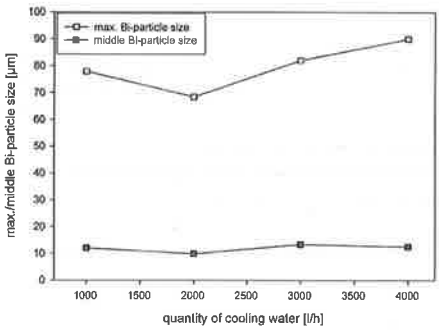

Figure 5: Influence of quantity of cooling water on the mean and maximum Bi-droplet in $AlZn_6Bi_8$ alloy

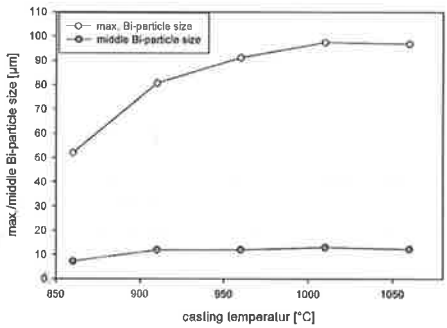

Figure 6: Influence of casting temperature on the mean and maximum Bi-droplet in $AlZn_6Bi_8$ alloy

Figure 5 shows the influence of the cooling water flow rate on the maximum and mean Bi-droplet size. For alloys which should reveal only small size maximum droplets, the optimum cooling water flow rate is around $Q = 2000$ l/hour for $T_{cast} = 960$ °C and $V_{cast} = 550$ mm/min. A smaller flow rate/cooling rate favors the droplet sedimentation, whereas a higher flow rate/ cooling rate Marangoni motion is encouraged.

Figure 6 shows the influence of the variation of casting temperature on the maximum and the mean Bi-droplet size. It is obvious that small casting temperatures lead to smaller temperature gradients ahead of the solidification front and thus higher viscosity of the parent melt. Therefore, the droplet motion is made difficult.

4 Simulation Part

4.1 Model Description

Because of the fact that in the present paper process modeling is of importance we skip a detailed model description. The reader is referred to the original papers of corresponding authors [5, 6]. Nevertheless, a brief description of most important model assumptions is given.

The used two phase model considers the parent alloy as the first, L_1, and the forming droplets as the second phase, L_2. During the monotectic reaction the monotectic matrix is transformed directly from L_1. Therefore, the solidification of monotectic matrix is modeled by increasing the L_1 viscosity and releasing latent heat on reaching the monotectic temperature. The decomposed L_2 droplets approaching the monotectic reaction front are modeled to be entrapped in the monotectic matrix by applying the same enlarged viscosity at or below the monotectic point. A similar approach is used by [1,6,10–12].

The model is based on solving the mass, momentum, species and enthalpy conservation equations for both liquids including droplet nucleation, solute redistribution and monotectic reaction [7]. Both Stokes and Marangoni motion is taken into account.

In addition to the above mentioned model considerations the following assumptions are made:

- Gravity-induced sedimentation is modeled with the Boussinesq approach.
- Both liquid phases are assumed to have the same viscosity.
- Collision and coagulation of droplets are not yet taken into account.
- Diffusion in a single droplet is thought to be infinite.

4.2 Geometry and Boundary Condition

For the process simulation of a binary $AlBi_{10}$ alloy a casting velocity of $V_{cast} = 828$ mm/min and a casting temperature of $T_{cast} = 792$ °C is considered. Due to the geometry of the casting a 2D symmetry has been chosen for the simulation. The mold is schematically shown in Figure 1 and in a 3D view in Figure 7. Here (①) indicates the copper mold, (②) indicates the used steel pouring nozzle on the top, (③) and (④) show the primary cooling zone, where (③) indicates the part of the mold where ideal contact is assumed and (④) the lower part where already solidification shrinkage and thermal contraction of the solid shells is considered. (⑤) indicates the position of the secondary cooling zone. In Figure 8 the applied boundary conditions are shown. (①) gives the position of the inlet, where a velocity inlet with the casting speed V_{cast} is considered. A heat transfer coefficient (HTC) of $h = 100$ W/m²K and a temperature of $T_{feed} = 682$ °C is considered for the steal feeder (②). (③) is divided in two parts: the upper part where $h = 1000$ W/m²K and $T_{mold} = 202$ °C and a lower part where $h = 100$ W/m²K and $T_{mold} = 202$ °C is used in order to model the start of the secondary cooling. For the rest of the secondary cooling (④) we have applied $h = 10000$ W/m²K and $T_{water} = 23$ °C. For the outlet (⑤), outflow is considered. A grid of 15960 cells and 16523 nodes is used.

The applied material properties are the same as used in [7]. Tab. 1 gives the values for the used thermodynamic properties of the system. As initial conditions, we start with hot melt ($T_{init} = 792$ °C) at rest ($V_{init} = 0$ m/min). Cooling and inflow are then resulting in an acceleration

of the melt in the strand, the formation of a solidifying shell and nucleation and growth of Bi-droplets.

4.3 Results and Discussion

Figure 9 shows three properties in the upper part of the casting, namely temperature field, volume fraction and density of the Bi-droplets 44s after switching on flow and cooling. The pictures are overlaid with two isothermal lines: binodal (T_b = 786 °C) and monotectic (T_m = 657 °C).

Table 1: Thermodynamic phase diagram used for the simulation

Monotectic temperature	T_m	930 K	657 °C
Monotectic concentration	c_m	0.47 at.%	3.526 wt.%
L_2 monotectic concentration	c_{L2}	83.4 at.%	97.493 wt.%
Critical Temperature	T_c	1310 K	1037 °C
Melting point of Al	T_f^A	933 K	660 °C
Melting point of Bi	T_f^B	543 K	270 °C
Gross concentration	c_0	1.415 at.%	10 wt.%
Slope of liquidus at c_0	m	148.1 K per at.%	20.42 °C per wt.%
Partitioning coefficient	k	51.72	9.55

The temperature field displayed in Figure 9a shows the temperature evolution from the upper border of the steel feeder (①) and to the end of the copper mold (② and ③). According to the experimental conditions, a gap between casting and copper mold is considered 15 mm below the steel feeder (③). This gap is indicated in Figure 9 by the white gap between mold and casting. The secondary cooling zone starts with that gap and moves on fare below the copper mold.

t = 10 s after switching on cooling und inflow, the temperature distribution reaches steady-state. The complicated boundary conditions applied for the considered strip caster lead to a temperature distribution (Figure 9 a) in the solidifying strand that has a strong temperature gradient

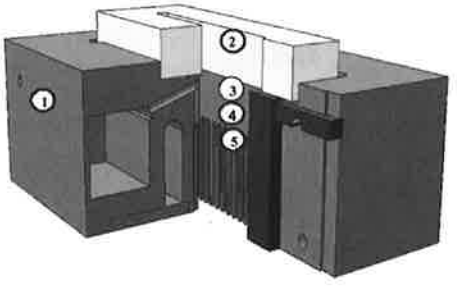

Figure 7: Casting Mold (described in the text)

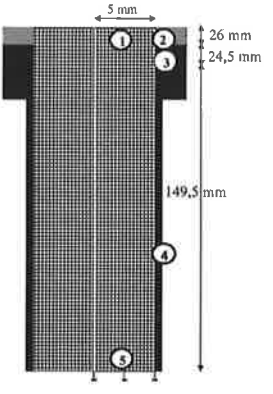

Figure 8: Geometry and boundary conditions (described in the text)

in the upper part of the copper mold (②). As the Marangoni force is proportional to the temperature gradient, the droplets which form along the wall are forced to move towards the centre of the strip (Figure 9 b). The movement of the droplets towards the centre of the strand is overlaid by Stokes motion and is therefore at the origin of two small vortices which occur at the wall (④).

Figure 9c shows the density, n, of the Bi-droplets. The black curve overlaid is the value of n along the strand at a depth of 25 mm ($n = 0$ is at the center of the figure). Due to the small temperature gradient in the steel feeder nucleation appears visible slightly below the binodal temperature (Figure 9c). It can be seen that the nucleation of the droplets is somewhat oscillatory in nature (⑤). At present, the origin of these oscillations is unclear. Zhoa [5] mentioned that oscillations appear in numerical calculations for describing the microstructure evolution in hypermonotectic alloys. The reasons therefore are changes in the supersaturation of the liquid caused by Marangoni and Stokes motion. Detail studies on that issue are ongoing.

5 Concluding Remarks

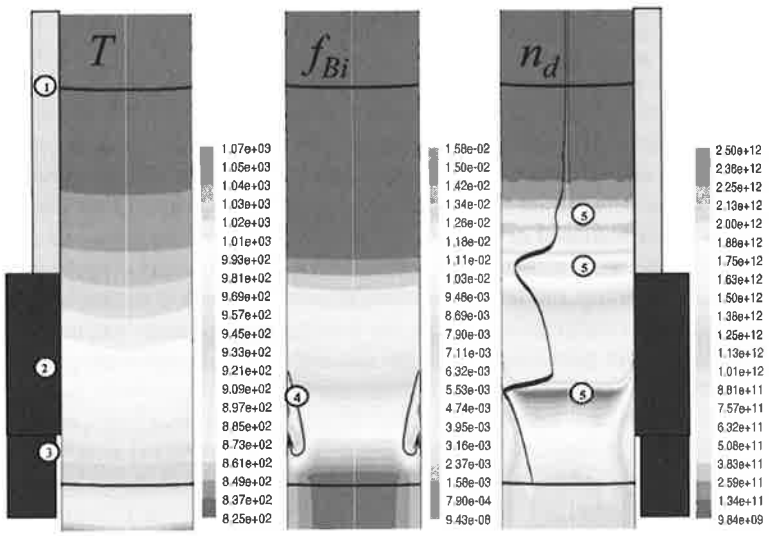

Figure 9: ① steel pouring nozzle, ② (ideal contact) and ③ start of the secondary cooling (air gap). (a) Temperature field with a strongest gradient in ②; (b) volume fraction: ④ indicates the position of high Marangoni motion towards the centre of the cast; (c) density of droplets: ⑤ indicates oscillatory in the droplet density. The black curve overlaid is the value of droplet density along the strand at a depth of 25 mm.

First results of investigations with ternary Al-Bi-Zn alloys have been presented in the first part of the paper, intended mainly to examine the influence of additional alloying elements, like Zn, and various process parameters. The results intend to show the following facts:

- Zn content variation has minor effect on the maximum and the mean Bi-droplet size compared to Bi-content variations.

- For the alloy $AlBi_8Zn_6$ the casting conditions which would result in the smallest maximum droplet size for T_{cast} = 960 °C have been found to be: a casting velocity of V_{cast} = 550 mm/min combined with a cooling water flow rate of Q = 2000 l/hour. For lower casting temperature the maximum droplet sizes can even been reduced.
- Further investigations are planed to evaluate the influence of different grain refiners, especially based on Al-Ti-C and Al-Ti-B, on the fineness of the minority phase distribution.

In the second part of the paper preliminary simulation results for a strip casting of AlBi10 have been presented. The complexity of the demixing process of hypermonotectic alloys together with the different boundary conditions particular for the considered caster make the qualitative interpretation of the results difficult.

However, the following statements can be made:

- The temperature field shows the highest gradient in the upper part of the copper mold.
- The Marangoni force increases with increasing temperature gradient which causes the motion of the Bi-droplets towards the centre of the strip.
- Oscillating droplet nucleation appears spatially in the strand. At present the reason for that is not clear. Maybe changing supersaturation in the liquid caused by Marangoni motion and Stokes sedimentation are of importance. Detail studies on that issue are ongoing.

6 Acknowledgements

This work was financially supported by the ESA-MAP project 'Solidification Morphologies of Monotectic Alloys-MONOPHAS'.

7 References

[1] L. Ratke, S. Diefenbach, Mater. Sci. Eng. 15, 1995, p. 263
[2] B. Predel et al, Decomposition of Alloys : The Early Stages, ed. Walter H. U., Ashhy M. F., Berlin: Springer, p. 517
[3] J. Moiseev, S. Vogelgesang, H. Zak, H. Palkowski, B Tonn, Metall 58, 2004, p. 289
[4] J. Moiseev, H. Zak, H. Palkowski, B. Tonn, Aluminium 81, 2005, p. 92
[5] J. Zhao, L. Ratke, Scripta Mater. 39, 1998, p.181
[6] J. Zhao, L. Ratke, Z. Metallkunde, 89, 1998, p. 241
[7] M.Wu, A. Ludwig, L. Ratke, Modell. Simul. Mater. Sci. Eng. 11, 2003, p. 755
[8] M.Wu, A. Ludwig, L. Ratke, Metall. Mater. Trans. 34A, 2003, p. 3009
[9] B. Prinz, DE Patent 40 03 018 A1, 1991
[10] J. Alkemper, L. Ratke, Z. Metall. 85, 1994, p. 365
[11] S. Diefenbach, Ph. D. Thesis Ruhr-Univercity Bochum, 1993
[12] L. Ratke et al., Materials and Fluid Under Low Gravity, ed L. Ratke et al. Berlin: Springer, 1995, p. 115